Chromium and tantalum site substitution patterns in Ni$_3$Al (L1$_2$) γ′-precipitates

Christopher Booth-Morrison,[1,a)] Zugang Mao,[1,b)] Ronald D. Noebe,[2] and David N. Seidman[1,3,c)]

[1]*Department of Materials Science and Engineering, Northwestern University, 2220 Campus Drive, Evanston, Illinois 60208-3108, USA*
[2]*NASA Glenn Research Center, 21000 Brookpark Rd., Cleveland, Ohio 44135, USA*
[3]*Northwestern University Center for Atom-Probe Tomography (NUCAPT), 2220 Campus Drive, Evanston, Illinois 60208-3108, USA*

The site substitution behavior of Cr and Ta in the Ni$_3$Al (L1$_2$)-type γ′-precipitates of a Ni–Al–Cr–Ta alloy is investigated by atom-probe tomography (APT) and first-principles calculations. Measurements of the γ′-phase composition by APT suggest that Al, Cr, and Ta share the Al sublattice sites of the γ′-precipitates. The calculated substitutional energies of the solute atoms at the Ni and Al sublattice sites indicate that Ta has a strong preference for the Al sites, while Cr has a weak Al site preference. Furthermore, Ta is shown to replace Cr at the Al sublattice sites of the γ′-precipitates, altering the elemental phase partitioning behavior of the Ni–Al–Cr–Ta alloy. © 2008 American Institute of Physics. [DOI: 10.1063/1.2956398]

Modern nickel-based superalloys are used in land-based and aerospace turbine engines at operating temperatures up to 1373 K. The high temperature strength and creep resistance of these alloys are due primarily to strengthening by the precipitated γ′-(L1$_2$) phase, which can accommodate substantial solute additions.[1] The mechanical properties of the γ′-phase depend on the sublattice site substitution behavior of these alloying additions,[2] motivating an investigation of the site occupancy of Cr and Ta in a model Ni–Al–Cr–Ta alloy that has been studied by atom-probe tomography (APT) and scanning electron miscroscopy.[3]

The addition of Cr to Ni–Al alloys reduces the lattice parameter misfit between the γ′-phase and the γ-matrix, often leading to spheroidal, nearly misfit-free γ′-precipitates.[4] Tantalum provides solid-solution strengthening and increases the volume fraction of the γ′-precipitate phase, thereby providing significant strengthening while improving γ′-phase stability and service life.[1] Previous APT,[5] atom-probe field-ion microscope,[6,7] and x-ray analysis experiments,[8–10] as well as results of first-principles calculations,[11–15] the cluster variation method,[16–18] and other techniques,[19–21] have indicated that Ta occupies the Al sublattice sites in ordered Ni$_3$Al. These findings contradict experimental results from ion channeling and nuclear-reaction analysis studies[22] and research based on short-range ordering employing pseudopotential approximations,[23] which claim that Ta occupies the Ni sublattice sites in Ni$_3$Al. The site preference of Cr has generally been found to depend on the alloy composition and aging treatment,[8,11,13,17,21,23,24] though some studies concluded that Cr occupies the Al sites, regardless of composition,[10] or temperature.[25]

We present APT results and first-principles calculations that elucidate the site substitution behavior of Cr and Ta in the γ′-phase of a Ni–Al–Cr–Ta superalloy aged at 1073 K. A Ni-10.0 Al-8.5 Cr-2.0 Ta at. % alloy was homogenized at 1573 K for 20 h, then annealed in the γ-phase field at 1503 K for 3 h, and water quenched. Ingot sections were aged at 1073 K under flowing argon for times ranging from 0.25 to 256 h, then water quenched, and microtip specimens were prepared for study by APT. Pulsed-laser APT data collection was performed at an evaporation rate of 0.04 ions pulse^{-1}, a specimen temperature of 40.0 ± 0.3 K, a pulse energy of 0.6 nJ pulse^{-1}, a pulse repetition rate of 200 kHz, and a gauge pressure of $< 6.7 \times 10^{-8}$ Pa. APT data were visualized and analyzed with IVAS™ 3.0 (Imago Scientific Instruments). Figure 1 shows an APT reconstruction that intersected a cuboidal γ′-precipitate in a sample aged for 256 h. The strong partitioning of Al and Ta, shown in black, to the γ′-phase, and Cr, in white, to the γ-phase is demonstrated.

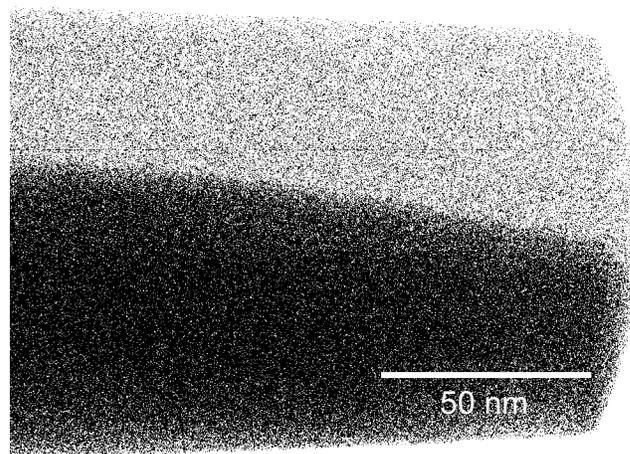The composition profiles across the γ′/γ interface in Fig. 1 are displayed in Fig. 2. The measured composition

FIG. 1. APT reconstruction of a cuboidal γ′-precipitate in a model Ni-10.0 Al-8.5 Cr-2.0 Ta at. % alloy aged at 1073 K for 256 h. The elements that partition to the γ′-precipitates, Al and Ta, are shown in black, while Cr, which partitions to the γ-matrix, is shown in white; Ni atoms are omitted for clarity.

a)Electronic mail: c-booth@northwestern.edu.
b)Electronic mail: z-mao2@northwestern.edu.
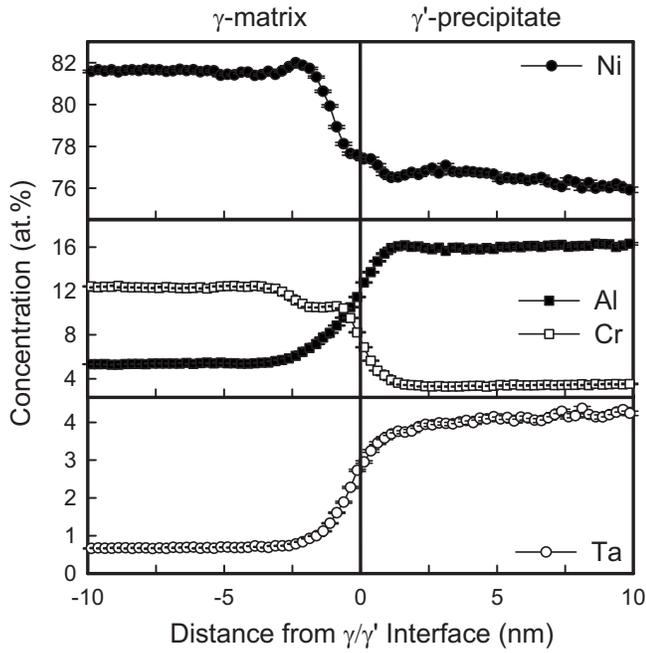c)Electronic mail: d-seidman@northwestern.edu

FIG. 2. The elemental concentration profiles across the γ'/γ interface for a Ni-10.0 Al-8.5 Cr-2.0 Ta at. % alloy aged at 1073 K for 256 h. Tantalum and Al partition to the γ'-precipitates, while Cr partitions to the γ-matrix.

of the γ'-precipitates is 75.37 ± 0.05 Ni- 16.56 ± 0.08 Al- 3.25 ± 0.09 Cr- 4.82 ± 0.09 Ta at. %, suggesting that Cr and Ta occupy the Al sites of the Ni$_3$Al γ'-precipitates. The relatively Cr rich γ'-precipitate composition of 76.49 ± 0.13 Ni- 17.47 ± 0.12 Al- 6.04 ± 0.07 Cr at. % measured for the reference Ni–Al–Cr alloy,[26,27] indicates that the addition of 2.0 at. % Ta leads to the preferential replacement of Cr by Ta in the γ'-precipitates.

First-principles calculations were performed to confirm the site substitution preferences of the solute atoms in the γ'-precipitates and to determine the thermodynamic driving force for the replacement of Cr by Ta atoms in the γ'-phase. The calculations employed the plane-wave pseudopotential total energy method with generalized gradient approximations,[28] as implemented in the Vienna *ab initio* simulation package (VASP),[29–31] using the projector augmented-wave potentials.[32] A plane wave cutoff energy of 300 eV and $8 \times 8 \times 8$ Monkhorst–Pack k-point grids were used, and found to be sufficient to give fully converged results. A three-dimensional periodic supercell with $2 \times 2 \times 2$ unit cells (32 atoms) was employed to determine the total energies of the cells, which converge to 2×10^{-5} eV atom^{-1}, while residual forces converge to 0.005 eV nm^{-1}. The Ni$_3$Al (L1$_2$) structure was fully relaxed, and the lattice parameter was determined to be 0.3566 nm, in good agreement with the experimental room temperature value of 0.3570 nm.[1]

The antisite formation energies associated with the Ni$_3$(Al$_{1-y}$Ni$_y$) and (Ni$_{1-x}$Al$_x$)$_3$Al structures were calculated and defined as

$$E_{\text{Ni}\to\text{Al}} = [E_{\text{Ni}_3(\text{Al}_{1-y}\text{Ni}_y)}^{\text{tot}} + \mu_{\text{Al}}] - [E_{\text{Ni}_3\text{Al}}^{\text{tot}} + \mu_{\text{Ni}}], \quad (1)$$

$$E_{\text{Al}\to\text{Ni}} = [E_{(\text{Ni}_{1-x}\text{Al}_x)_3\text{Al}}^{\text{tot}} + \mu_{\text{Ni}}] - [E_{\text{Ni}_3\text{Al}}^{\text{tot}} + \mu_{\text{Al}}], \quad (2)$$

where μ_i is the chemical potential per atom of the bulk element i assuming same cell symmetry, and are -5.432

TABLE I. Total E^{tot} and substitutional $E_{Z\to\text{Ni,Al}}$ energies determined by first-principles calculations. (For these calculations $x=0.042$, $y=0.125$, and $Z=\text{Cr, Ta}$.)

	E^{tot} (eV)	$E_{Z\to\text{Ni,Al}}$ (eV atom^{-1})
Ni$_3$Al	-174.944	$\cdots$
(Ni$_{1-x}$Cr$_x$)$_3$Al	-177.966	0.648
Ni$_3$(Al$_{1-y}$Cr$_y$)	-179.748	0.565
(Ni$_{1-x}$Ta$_x$)$_3$Al	-180.957	0.033
Ni$_3$(Al$_{1-y}$Ta$_y$)	-183.198	-0.473

and -3.697 eV atom^{-1} for Ni and Al, respectively. The antisite formation energies are $E_{\text{Ni}\to\text{Al}}=0.986$ eV atom^{-1} and $E_{\text{Al}\to\text{Ni}}=0.742$ eV atom^{-1}, and are energetically unfavorable. Other first-principles studies have found that the antisite formation energies are similar and range from 0.51 to 0.99 eV.[33–35] Another investigation calculated the Al and Ni antisite energies to be -0.92 and 2.04 eV, respectively.[15]

Four substitutional structures, (Ni$_{1-x}$Cr$_x$)$_3$Al, Ni$_3$(Al$_{1-y}$Cr$_y$), (Ni$_{1-x}$Ta$_x$)$_3$Al, and Ni$_3$(Al$_{1-y}$Ta$_y$), were modeled by substituting one Cr or Ta atom at one of the Ni or Al sublattice sites. Table I summarizes the calculated total energies of the relaxed structures E^{tot} and the substitutional energies, $E_{Z\to\text{Ni}}$ and $E_{Z\to\text{Al}}$, ($Z=\text{Cr, Ta}$), which are defined as follows:

$$E_{Z\to\text{Ni}} = [E_{(\text{Ni}_{1-x}Z_x)_3\text{Al}}^{\text{tot}} + \mu_{\text{Ni}}] - [E_{\text{Ni}_3\text{Al}}^{\text{tot}} + \mu_Z], \quad (3)$$

$$E_{Z\to\text{Al}} = [E_{\text{Ni}_3(\text{Al}_{1-y}Z_y)}^{\text{tot}} + \mu_{\text{Al}}] - [E_{\text{Ni}_3\text{Al}}^{\text{tot}} + \mu_Z], \quad (4)$$

where the chemical potentials of Cr and Ta are -9.103 and -11.478 eV atom^{-1}, respectively. The calculated results demonstrate that Ta atoms *strongly* prefer to occupy the Al sublattice sites of Ni$_3$Al, as $E_{\text{Ta}\to\text{Al}}$ is significantly smaller than $E_{\text{Ta}\to\text{Ni}}$. Chromium *weakly* prefers to substitute at the Al sites, as $E_{\text{Cr}\to\text{Al}}$ is only slightly smaller than $E_{\text{Cr}\to\text{Ni}}$. The substitutional energy associated with the replacement of Cr atoms by Ta atoms on the Al sublattice sites of the Ni$_3$Al structure is calculated as follows:

$$E_{\text{Ta}\to\text{Cr}} = [E_{\text{Ni}_3(\text{Al}_{1-y}\text{Ta}_y)}^{\text{tot}} + \mu_{\text{Cr}}] - [E_{\text{Ni}_3(\text{Al}_{1-y}\text{Cr}_y)}^{\text{tot}} + \mu_{\text{Ta}}], \quad (5)$$

and is -1.038 eV atom^{-1} Thus the replacement of Cr by Ta in the γ'-precipitates is energetically favorable, and is observed by APT to occur.

To verify that the substitutional patterns of Cr modeled herein result in the lowest energy configurations, two other substitutional patterns (Ni$_{1-x}$Al$_x$)$_3$(Al$_{1-y}$Cr$_y$) and (Ni$_{1-x}$Cr$_x$)$_3$(Al$_{1-y}$Ni$_y$) were modeled. These structures may form by the occupation of a Ni or Al sublattice by a Cr atom, and the displacement of the Ni or Al atom to an antisite. These structures are also found to be energetically unfavorable, yielding formation energies of 1.138 and 1.337 eV atom^{-1} for (Ni$_{1-x}$Al$_x$)$_3$(Al$_{1-y}$Cr$_y$), and (Ni$_{1-x}$Cr$_x$)$_3$(Al$_{1-y}$Ni$_y$), respectively.

The local stresses and strains due to site substitution result in the average atomic forces and displacements at the first nearest-neighbor distance displayed in Table II. We note that no atomic force was measured for relaxed Ni$_3$Al prior to site substitution. The substitution of Ta at the Al sublattice sites results in smaller values of the atomic force and displacement than substitution of Ta at the Ni sites. The atomic

TABLE II. Average atomic forces and displacements at the first nearest-neighbor distance from first-principles calculations for four different substitutional structures.

	Average atomic force (eV A^{-1})	Average atomic displacement (A)
$(Ni_xCr_{1-x})_3Al$	0.0150	0.0294
$Ni_3(Al_yCr_{1-y})$	0.0112	0.0325
$(Ni_xTa_{1-x})_3Al$	0.0154	0.0479
$Ni_3(Al_yTa_{1-y})$	0.0095	0.0215

forces and displacements associated with Cr substitution at the Ni and Al sites are comparable, providing supporting evidence that Cr only *weakly* prefers Al sublattice sites.

From APT results, the addition of Ta to a Ni–Al–Cr alloy leads to the rejection of Al and Cr from the γ'-precipitates, though the effect is more pronounced for Cr. The elemental phase partitioning behavior is quantified by the partitioning ratio, $K_i^{\gamma'/\gamma}$; the ratio of the concentration of an element i in the γ'-precipitates to the concentration of the same element in the γ-matrix. A 2.0 at. % addition of Ta to a Ni-10.0 Al-8.5 Cr at. % alloy, aged at 1073 K for 256 h, decreases the value of $K_{Al}^{\gamma'/\gamma}$ from 3.17 ± 0.01 to 2.20 ± 0.02, and the value of $K_{Cr}^{\gamma'/\gamma}$ from 0.63 ± 0.01 to 0.26 ± 0.03. The value of $K_{Ta}^{\gamma'/\gamma}$ for the Ni–Al–Cr–Ta alloy at 256 h is 10.25 ± 0.07, and the partitioning of Ni is unaffected by the addition of Ta.

To conclude, Ta and Cr substitute preferentially at the Al sublattice sites in Ni_3Al ($L1_2$). The substitution of Ta for Al is energetically favorable, while the substitution of Cr for Al is less so. This results in the replacement of Cr by Ta at the Al sublattice sites and in the γ'-precipitates, and alters the partitioning behavior of the elements in the Ni–Al–Cr–Ta alloy.

[1]R. C. Reed, *The Superalloys: Fundamentals and Applications* (Cambridge University Press, New York, 2006), p. 372.
[2]R. D. Rawlings and A. E. Staton-Bevan, J. Mater. Sci. **10**, 505 (1975).
[3]C. Booth-Morrison, R. D. Noebe, and D. N. Seidman, *Proceedings of the International Symposium of Superalloy*, 2008 (unpublished).
[4]A. Taylor and W. Floyd, J. Inst. Met. **81**, 451 (1952).
[5]D. Blavette and A. Bostel, Acta Metall. **32**, 811 (1984).
[6]M. K. Miller, R. Jayaram, L. S. Lin, and A. D. Cetel, Appl. Surf. Sci. **76**, 172 (1994).
[7]K. L. More and M. K. Miller, J. Phys. C **11**, 391 (1988).
[8]S. Ochiai, Y. Oya, and T. Suzuki, Acta Metall. **32**, 289 (1984).
[9]A. V. Karg, D. E. Fornwalt, and O. H. Kriege, J. Inst. Met. **99**, 301 (1971).
[10]A. Chiba, D. Shindo, and S. Hanada, Acta Metall. Mater. **39**, 13 (1991).
[11]A. V. Ruban and H. L. Skriver, Phys. Rev. B **55**, 856 (1997).
[12]S.-Y. Wang, C.-Y. Wang, J.-H. Sun, W.-H. Duan, and D.-L. Zhao, Phys. Rev. B **65**, 035101 (2002).
[13]M. H. F. Sluiter and Y. Kawazoe, Phys. Rev. B **51**, 4062 (1995).
[14]S. Raju, E. Mohandas, and V. S. Raghunathan, Scr. Mater. **34**, 1785 (1996).
[15]C. Jiang and B. Gleeson, Scr. Mater. **55**, 433 (2006).
[16]H. Murakami, Y. Koizumi, T. Yokokawa, Y. Yamabe-Mitarai, T. Yamagata, and H. Harada, Mater. Sci. Eng., A **A250**, 109 (1998).
[17]M. Enomoto and H. Harada, Metall. Trans. A **20A**, 649 (1989).
[18]Y. P. Wu, N. C. Tso, J. M. Sanchez, and J. K. Tien, Acta Metall. **37**, 2835 (1989).
[19]E. S. Machlin and J. Shao, Scr. Metall. **11**, 859 (1977).
[20]R. W. Guard and J. H. Westbrook, Trans. AIME **215**, 807 (1959).
[21]Y. Saito and H. Harada, Mater. Sci. Eng., A **A223**, 1 (1997).
[22]H. Lin, L. E. Seiberling, P. F. Lyman, and D. P. Pope, *High-Temperature Ordered Intermetallic Alloys II*, MRS Symposia Proceeding No. 81 (Materials Research Society, Pittsburgh, 1987), p. 165.
[23]A. O. Mekhrabov, M. V. Akdeniz, and M. M. Arer, Acta Mater. **45**, 1077 (1997).
[24]M. P. Arbuzov, E. T. Kachkovskaya, and B. V. Khaenko, Fiz. Met. Metalloved. **21**, 854 (1966).
[25]C. Jiang, D. J. Sordelet, and B. Gleeson, Acta Mater. **54**, 1147 (2006).
[26]C. K. Sudbrack, D. Isheim, R. D. Noebe, N. S. Jacobson, and D. N. Seidman, Microsc. Microanal. **10**, 355 (2004).
[27]C. K. Sudbrack, T. D. Ziebell, R. D. Noebe, and D. N. Seidman, Acta Mater. **56**, 448 (2008).
[28]J. P. Perdew, *Electronic Structure of Solids* (Akademie, Berlin, 1991), Vol. 11.
[29]G. Kresse and J. Furthmueller, Phys. Rev. B **54**, 11169 (1996).
[30]G. Kresse and J. Furthmuller, Comput. Mater. Sci. **6**, 15 (1996).
[31]G. Kresse and J. Hafner, Phys. Rev. B **49**, 14251 (1994).
[32]G. Kresse and D. Joubert, Phys. Rev. B **59**, 1758 (1999).
[33]D. Vogtenhuber, J. Houserova, W. Wolf, R. Podloucky, W. Pfeiler, and W. Pueschl, *Integrative and Interdisciplinary Aspects of Intermetallics*, MRS Symposia Proceeding No. 842 (Materials Research Society, Pittsburgh, 2005), p. 541.
[34]C. L. Fu and G. S. Painter, Acta Mater. **45**, 481 (1997).
[35]H. Schweiger, O. Semenova, W. Wolf, W. Puschl, W. Pfeiler, R. Podloucky, and H. Ipser, Scr. Mater. **46**, 37 (2002).